Supporting Information

Park et al. 10.1073/pnas.1213508110

SI Discussion

Comments on STAU2 Tethering Results. For reasons that remain unclear, our tethering results do not recapitulate those of others. Tethering rat Staufen (STAU)[52] downstream of the termination codon of β-globin 4boxB reporter mRNA was reported to reduce reporter mRNA abundance by only ∼25% in HeLa cells (1). Additional HeLa cell data claiming that renilla luciferase (RLUC) activity from an RLUC-8xMS2bs reporter mRNA was reduced by ∼10% or ∼30% when, respectively, MS2-tagged rat STAU2[59] or MS2-tagged rat STAU1[55] was expressed compared with when MS2 alone was expressed (2) may be problematic because there was no control using an RLUC reporter mRNA that did not contain the MS2bs tethering sites, and there was no quantitation of reporter mRNA levels and, therefore, RLUC activity was not normalized to the level of the mRNA from which it derived. Currently, there is no reason to think that rat STAU isoforms would function differently than human STAU isoforms. Rat and human STAU1 and STAU2 isoforms share ∼92% and ∼93% identity, respectively.

SI Materials and Methods

Plasmid Constructions. To construct pCI-neo-HA_3, which encodes three tandem HA tags, the HA_3 region of pSTAU1-HA_3 (3, 4) was PCR-amplified using two primers: 5′-ATAGAATTCATG-ATCTTTTACCCATACGAT-3′ (sense) and 5′-ATAGGGCCC-TCTAGATTATCA-3′ (antisense), where underlined nucleotides specify EcoRI and XbaI sites, respectively. The resulting PCR fragment was digested with EcoRI and XbaI and inserted into pCI-neo (Promega) that had been digested with EcoRI and XbaI.

To generate pCI-neo-STAU1[55]-HA_3, pCI-neo-STAU2[62]-HA_3, and pCI-neo-STAU2[59]-HA_3, each of which encodes a STAU isoform with a C-terminal HA_3 tag, pCI-neo was digested with EcoRI and, after making the ends blunt using Klenow fragment (New England Biolabs), with XbaI. The resulting vector was ligated to fragments from pSTAU1[55]-HA_3, pcDNA-STAU2[62]-HA_3, or pcDNA-STAU2[59]-HA_3. These fragments were generated using KpnI, the resulting ends of which were made blunt using Klenow, and then XbaI.

pcDNA-STAU2[62]-HA_3 or pcDNA-STAU2[59]-HA_3 was generated from pSTAU1[55]-HA_3 that had been digested with KpnI and NotI, and the resulting vector fragment was ligated to a fragment containing human STAU2[62] or STAU2[59] cDNA that had been digested with KpnI and NotI. STAU2[62] or STAU2[59] cDNA was obtained by PCR-amplifying reverse-transcribed HeLa-cell RNA using, respectively, the sense primer 5′-GCTTGGTACCTGCA-CTGTGCATGGCAAACCCAAAAGAG-3′ or 5′-GCTTGGTA-CCTGCACTGTGCATGCTTCAAATAAATCAG-3′ and the common antisense primer 5′-AAAGATGCGGCCGCTGACG-GCCGAGTTTGATTTC-3′, where underlined nucleotides specify a KpnI or NotI site, respectively.

For the bacterial production of human STAU2[62] or STAU2[59] that harbors an N-terminal GST tag, pGST-STAU2[62] or pGST-STAU2[59] was constructed by ligating the SalI-NotI vector fragment from pGEX-4T-1 (GE Healthcare) to a PCR-amplified fragment that had been digested with SalI and NotI. PCR fragments were generated using pcDNA-STAU2[62]-HA_3 or pcDNA-STAU2[59]-HA_3, the sense primer 5′-GGTCGACTCACCATGG-CAAACCCAAA-3′ or 5′-GGTCGACTCACCATGCTTCAAA-TAA-3′, respectively, and the common antisense primer 5′-TATAGCGGCCGCCTAGACGGCCGAG-3′, where underlined nucleotides specify a SalI or NotI site, respectively. To enable removing the GST tag from GST-STAU2[62] using PreScission Protease, pGEX-6P-2-STAU2[62] was constructed by ligating the BamHI-NotI vector fragment from pGEX-6P-2 (GE Healthcare) to BamHI-NdeI and NdeI-NotI fragments from pGST-STAU2[62].

For the bacterial production of human STAU2[62] or STAU2[59] that harbors a C-terminal 6xHIS tag, pSTAU2[62]-HIS or pSTAU2[59]-HIS was constructed by ligating the NcoI-KpnI vector fragment from pETDUET-1 (Novagen) to a PCR-amplified fragment that had been digested with NcoI and KpnI. PCR fragments were generated using pcDNA-STAU2[62]-HA_3 or pcDNA-STAU2[59]-HA_3, the sense primers 5′- CATCCATGGATGGCAAACCCAAAA-GAG-3′ or 5′- CATCCATGGATGCTTCAAATAAATCAG-3′, respectively, and the common antisense primer 5′-GGTACCT-TAGTGGTGGTGGTGGTGGTGCTCGACGACGGCCGAG-TTTGATTTCTTG-3′, where underlined nucleotides specify a NcoI or KpnI site, respectively.

For the bacterial production of human STAU2[62] or STAU2[59] that harbors a C-terminal GST tag, pSTAU2[62]-GST or pSTAU2[59]-GST was constructed by ligating the EcoRI-PacI vector fragment from pSTAU2[62]-HIS or pSTAU2[59]-HIS to a fragment that had been digested with EcoRI and NotI from pcDNA-STAU2[62]-HA_3 or pcDNA-STAU2[59]-HA_3, respectively, and a PCR-amplified GST fragment that had been digested with NotI and PacI. PCR fragments were generated using pGEX-4T-1, the sense primer 5′-AAAGATGCGGCCGCATGTCCCCTATACTAGG -3′, and antisense primer 5′- CCTAGGTTAATTAACTAATCCGATTTTG-GAGGATG -3′, where underlined nucleotides specify a NotI or PacI site, respectively.

To construct pMS2-HA-STAU2[62] or pMS2-HA-STAU2[59], which encode full-length human STAU2[62] or STAU2[59] followed successively by an N-terminal oligomerization-defective MS2 coat protein (3) and an HA tag, pMS2-HA-STAU1[55] (3) was digested with NheI followed by dephosphorylation using Antarctic phosphatase (New England BioLabs), and the resulting vector fragment was ligated to a PCR-amplified fragment containing human STAU2[62] or STAU2[59] cDNA that had been digested with NheI. STAU2[62] or STAU2[59] cDNA was PCR-amplified using pcDNA-STAU2[62]-HA_3 or pcDNA-STAU2[59]-HA_3, respectively, the sense primer 5′-GCTAGCATGGCAAACCCAAAAGAGAAAA-CTGC-3′ or 5′-GCTAGCATGCTTCAAATAAATCAGATGTT-CTCAGTGCAGC-3′, respectively, and the common antisense primer 5′-ATGCTAGCTTGACGGCCGAGTTTGATTTC -3′, where underlined nucleotides specify an NheI site.

To generate pMS2-HA-STAU1[55R], which is resistant to down-regulation by STAU1 siRNA, site-directed mutagenesis was performed using Pfu Turbo DNA polymerase (Stratagene), the sense primer 5′-CTTACTCTCGGATGCAGTCCACATATAA-TTATAATATGAGAGGAGGTGCTTATCCCC-3′, and the antisense primer 5′-GGGGATAAGCACCTCCTCTCATATTA-TAATTATATGTGGACTGCATCCGAGAGTAAG-3′, where underlined nucleotides denote silent-codon changes that distinguish the encoded transcript from the cellular transcript. pMS2-HA-STAU2[62R] or pMS2-HA-STAU2[59R], which is resistant to down-regulation by STAU2 siRNA, was constructed as described above, except that the sense primer was 5′-GCGCAAATTCA-ACAGGCCAAAAAAGAGAAGGAACCGGACTATGTTTT-GCTTTCAGAAAG-3′ and the antisense primer was 5′-CTT-TCTGAAAGCAAAACATAGTCCGGTTCCTTCTCTTTTTT-GGCCTGTTGAATTTGCGC-3′, where underlined nucleotides denote silent-codon changes that distinguish the encoded transcript from the cellular transcript.

For the bacterial production of human UPF1 or UPF1(G495R, G497E) that harbors an N-terminal GST tag, pGEX-6P-1-UPF1 (115-914) or pGEX-6P-1-UPF1(G495R,G497E) was constructed by ligating the BamHI-EcoRI vector fragment from pGEX-6P-1 (GE Healthcare) to a PCR-amplified fragment that had been digested with BamHI and EcoRI. PCR fragments were generated using pCMV-MYC-UPF1 (3) or pCMV-MYC-UPF1(G495R, G497E) (5), the sense primer 5′-AAAAGGATCCACGAAGGACCTCCCCATACAC-3′, and the antisense primer 5′-AAAAGAATTCTTATCAGCTGAACTGCATGAGGC-3′, where underlined nucleotides specify a BamHI or EcoRI site, respectively.

Notably, pCMV-MYC-UPF1(G495R,G497E) (5) contains an additional mutation, P486S, that resides outside of the ATP-binding pocket.

Cell Transfection and Lysis and Protein and RNA Purification. Human HeLa, HEK293T, or HeLa Tet-Off Advanced (Clontech) cells were grown in DMEM (GIBCO-BRL) containing 10% FBS (GIBCO-BRL) and transiently transfected with STAU1 siRNA (3), STAU2 siRNA (5′-AGGAAAAGGAGCCGGAUUAdTdT-3′; Thermo Fisher Scientific), STAU2(A) siRNA, which consists of a single siRNA (Thermo Fisher Scientific), STAU2(B), which is a mixture of four siRNAs (ON-TARGETplus SMARTpool STAU2 siRNA; Thermo Fisher Scientific), UPF1 siRNA (3), or a nonspecific Control siRNA (3) using Oligofectamine (Invitrogen) and/or the specified plasmids using Lipofectamine 2000 Reagent (Invitrogen). Human neuroblastoma SK-N-MC cells were grown in MEM (GIBCO-BRL) containing 10% (vol/vol) FBS, 1 mM sodium pyruvate, 1% (wt/vol) nonessential amino acids, and 4 mM L-glutamine. mRNA half-life measurements using the HeLa Tet-Off Advanced cells and 2 μg/mL of doxycycline (Calbiochem) were as previously described (6). Cells were lysed using Passive Lysis Buffer (Promega), and protein was isolated. RNA was purified using TRIzol Reagent (Invitrogen).

Immunoprecipitations (IPs) (7) used anti-FLAG (Sigma), anti-HA (Roche), mouse IgG (Sigma), or rat IgG (Sigma). Where specified, HeLa cells were cross-linked before IP using formaldehyde, quenched using glycine, and lysed using sonication (8). After IP, cross-links were reversed by heating (8).

For Western blotting (WB), protein was electrophoresed in SDS-polyacrylamide, transferred to a PVDF membrane (Amersham), and probed with an antibody that recognizes STAU1 (7); STAU2, FLAG, or β-Actin (Sigma); Calnexin (StressGen); HA (Roche); UPF1 (8); UPF2, PLCγ1, or RPL10 (Santa Cruz Biotechnologies); PABPC1 (9); GST (GE Healthcare); and MYC (Calbiochem). Immunoreactivity was assessed using SuperSignal West Pico or Femto (Thermo Fisher Scientific). Films were quantitated using ImageQuant 5.2 (Molecular Dynamics).

RT-PCR. Reverse transcription and PCR amplifications were as described previously (7) using the following primer pairs. FLUC-GAP43 3′ UTR, FLUC-SERPINE1 3′ UTR, FLUC-c-JUN SBS, FLUC-ARF1 SBS, or FLUC-FLJ21870 3′ UTR mRNA was amplified using the primer pair 5′-AATACGACTCACTATAGGGA-3′ (sense) and, respectively, 5′-TGGAAAGCCATTTCTTAGAG-3′ (antisense), 5′-TGAAGGCGTCTTTCCCCAGG-3′ (antisense), 5′-AGGCAGGCCAGAAAGAGTTC-3′ (antisense), 5′- TCCTGGTGAGAAGTCTCC-3′ (antisense), or 5′-GGTACTGGGAGGCCTTTTTC -3′ (antisense). Cellular GAP43 pre-mRNA or GAPDH mRNA was amplified using the primer pairs 5′-CCACAAAATGTTTCTTTCACACATA-3′ (sense) and 5′-TTACAGCTAAATCTAGGCGTCACAT-3′ (antisense), or 5′-CAAGATCATCAGCAATGCC-3′ (sense) and 5′-CTGTGGTCATGAGTCCTTCC-3′ (antisense), respectively. GAP43, MUP, SMG7, FLUC, FLUC-MS2bs, and RLUC mRNA was amplified as described previously (3). TRE-FLUC-SERPINE1 3′ UTR mRNA was amplified as described previously (6). RT-PCR products were electrophoresed in 5% (wt/vol) polyacrylamide and quantitated using a Typhoon 9410 Variable Mode Imager and ImageQuant 5.2 (Molecular Dynamics).

RT-qPCR. RT coupled to real-time quantitative (q)PCR was performed using the Fast SYBR Green master mix (Applied Biosystems) and 7500 Real-Time PCR System (Applied Biosystems). GAPDH, GAP43, SERPINE1, ARF1, or IL7R mRNA and GAP43, SERPINE1, ARF1, or IL7R pre-mRNA were amplified using the primer pair 5′-CTTCCTCTTGTGCTCTTG-3′ (sense) and 5′-CTTCCTCTTGTGCTCTTG-3′ (antisense), 5′-GATGAGGTTTGATTTGAACTTC-3′ (sense) and 5′-ATCCTTCTTCTCTCCTTTGA-3′ (antisense), 5′-GAGAAGAACCAAACAGGTTG-3′ (sense) and 5′-GGGCTTCATCCTTCTTATTAG-3′ (antisense), 5′-GCTCAGACCAACAAGTTC-3′ (sense) and 5′-GTCATTCCCAGGTTCTCT-3′ (antisense), 5′-TTATTACTTCAGAACTCCAGAGAT-3′ (sense) and 5′-GCCAAGATGACCAACAGA-3′ (antisense), 5′-GCCACTACTTCCAGAACA-3′ (sense) and 5′-CAGTCCAGTCCTTCATAGAG-3′ (antisense), 5′-AAAGAAAGAACGAACGAACC-3′ (sense) and 5′-AACAGATGTGGATACAGGATTA-3′ (antisense), 5′-CCCATGACCATTTGACACT-3′ (sense) and 5′-CACTGGCTCCTCACATTC-3′ (antisense), 5′-ACTCCTACCTGAATCAAGAC-3′ (sense) and 5′-GCTATTATCTATTGCCAGTTGT-3′ (antisense), respectively.

Recombinant Protein Purification. GST-STAU1^{55} (3), GST-STAU2^{62}, GST-STAU2^{59}, STAU2^{62}-GST, STAU2^{59}-GST, GST-PABPC1, GST-UPF1, and GST-UPF1(G495R,G497E) (the last two of which consisted of UPF1 amino acids 115–914), HIS-STAU1^{55} (3), STAU2^{62}-HIS, and STAU2^{59}-HIS were individually produced in *Escherichia coli* BL21 DE3. All GST-tagged proteins were subsequently affinity-purified using a GSTrap HP column (GE Healthcare). PreScission Protease (GE Healthcare) was used to cleave the GST tag from GST-STAU2^{62}, GST-PABPC1, GST-UPF1, and GST-UPF1(G495R,G497E). Cleaved proteins were passed over the GSTrap HP column again to remove GST and PreScission Protease. UPF1 or UPF1(G495R,G497E) were additionally purified by gel filtration using a 120-mL HiLoad Superdex 200 16/60 prep-grade column (GE Healthcare). All HIS-tagged proteins were purified using a HisTrap FF column (GE Healthcare). HIS-STAU1^{55} was additionally purified by cation exchange chromatography using a HiTrap SP FF column (GE Healthcare). SYPRO Ruby Protein Gel Stain (Lonza) and Coomassie Blue (Sigma) were used to determine protein purity and amount.

For isolation of polysome pellets, SK-N-MC cells (2×10^7) were treated with 10 μg/mL of cycloheximide at 37 °C for 15 min, harvested, and then lysed using polysome extraction buffer (10). After centrifugation at 13,000 × *g* at 4 °C for 10 min, polysome pellets and the corresponding supernatant were generated by centrifugation at 291,000 × *g* in an SW60 rotor (Beckman) at 4 °C for 2 h. Pellets were resuspended in ribosome lysis buffer.

In Vitro Pull-Down Assays. Baculovirus-produced and purified FLAG-UPF1 (11) was incubated with Anti-FLAG-M2 Affinity Gel (Sigma) at 4 °C for 1 h, mixed with GST-STAU1^{55}, GST-STAU2^{62}, GST-STAU2^{59}, or GST-PABPC1 and incubated at 4 °C for an additional hour. The resin was washed five times using NET2 buffer (12). Bound proteins were eluted by boiling in 1× SDS sample buffer (12) and subjected to WB.

GST-STAU1^{55} was added to glutathione Sepharose 4B resin (GE Healthcare), incubated at 4 °C for 1 h, mixed with an equal amount of HIS-STAU1^{55}, STAU2^{62}-HIS, STAU2^{59}-HIS, or BSA, and incubated at 4 °C for an additional hour. Beads were washed five times using pull-down buffer [20 mM Hepes (pH 7.9), 150 mM NaCl, 0.5 mM EDTA, 10% (vol/vol) glycerol, 0.1% Triton X-100, and 1 mM DTT]. Bound proteins were eluted by boiling in 1× SDS sample buffer, electro-

phoresed in SDS-polyacrylamide (8% wt/vol), and stained using SYPRO Ruby Protein Gel Stain solution (Lonza).

STAU2^{62}-HIS or STAU2^{59}-HIS was added to Ni-NTA Magnetic Agarose Beads (Qiagen), incubated at 4 °C for 1 h, mixed with an equal amount of GST-STAU1^{55}, STAU2^{62}-GST, STAU2^{59}-GST, or GST-PABPC1, and incubated at 4 °C for 1 h. The beads were washed five times using NPI-20-Tween buffer (Qiagen). Bound proteins were eluted using elution buffer [50 mM Hepes (pH 7.4), 500 mM NaCl, 500 mM imidazole, and 5% glycerol], boiled in 1× SDS sample buffer, and subjected to WB.

In Vitro ATPase Assays. Reactions were performed as previously described (13), except the pH of the ATPase buffer was 7. Reactions (20 μL) were stopped after 1 h by the addition of 400 μL of ice-cold 10% (wt/vol) acid-washed charcoal (Sigma) in 10 mM EDTA and incubated for an additional 1 h on ice. After centrifugation at 18,800 × *g* for 5 min, the [^{32}P] in 100 μL of supernatant was quantitated using the Cerenkov method.

In Vitro Helicase Assays. To generate the RNA–DNA duplex (13), a 44-nt RNA was transcribed in vitro using MEGAscript (Ambion) T7 RNA polymerase. An 18-nt DNA (Integrated DNA Technologies) was 5′-γ-[^{32}P]-labeled using T4 polynucleotide kinase (New England Biolabs). Gel-purified RNA was subsequently annealed to γ-[^{32}P]-labeled DNA (14). Helicase assays were as previously described (14), except they were performed at pH 7 in the presence or absence of 0.5 mM or 2 mM of ATP, ADPNP, or ADP, 0.25 nM of γ-[^{32}P]-labeled RNA–DNA duplex, and the specified amount of UPF1, HIS-STAU1^{55}, STAU2^{62}, STAU2^{59}-HIS, or PABPC1. Samples were taken after incubating at 37 °C for 1 h. ADP-BeF_3^- was a mixture of BeF_2 and potassium fluoride (KF) in, respectively, fivefold and 25-fold molar excess relative to ADP, ADP-VO_3^-, or ATP +$NAVO_3$ was a mixture of $NaVO_3$ in fivefold molar excess relative to, respectively, ADP or ATP. Reactions were terminated by the addition of 5× Helicase Stop Buffer, which contained 100 mM EDTA, 50% (vol/vol) glycerol, 0.5% SDS, 0.05% bromophenol blue, and 0.05% xylene cyanol blue. Samples were electrophoresed in 16% (wt/vol) polyacrylamide, and radioactivity was visualized using phosphorimaging.

RNase Protection Assays. The α-[^{32}P]UTP-labeled 60-nt GGG $(CU)_{28}$C RNA was generated, and RNase protection assays were performed as described by Bonneau et al. (15) with the following modifications. Reactions (20 μL) contained helicase-assay buffer (pH 7), 10% (vol/vol) glycerol, and 5 pmol of α-[^{32}P]UTP-labeled 60-mer RNA. Amounts of additional constituents were as follows: 10 pmol of UPF1; 40 pmol of STAU2^{62}; 2 mM of ATP, ADP, or ADPNP; 10 mM of $NaVO_3$ or AlF_3; or 50 mM of KF. After 1 h at 4 °C, 1.1 μL of an RNase solution containing 1 μg of RNase A (Sigma) and 1 U of RNase T1 (Ambion) were added to each reaction, and the incubation was continued for 20 min at 20 °C. Reactions were terminated with the addition of 200 μL of TRIzol. Samples were extracted using phenol-chloroform, precipitated using 2-propanol, washed using 75% (vol/vol) ethanol, dried at 43.5 °C, and dissolved in 15 μL of a mixture of one part distilled water and two parts Gel Loading Buffer II (Ambion). Samples were heated for 3 min at 95 °C before loading. The Decade Marker (Ambion) was γ-[^{32}P]-labeled to serve as size standards. Samples were separated in 7 M urea and 22% (wt/vol) acrylamide (19:1 acrylamide:bis). The gel was analyzed without drying using phosphorimaging. Half-volumes were loaded for samples not treated with RNase.

EMSAs. Reactions (20 μL), which contained the same components as did the helicase assays except they lacked ATP, were performed at 37 °C for 1 h (details in Fig. S4), after which 50% vol/vol glycerol (5 μL) was added. Samples were electrophoresed in 5% (wt/vol) polyacrylamide at 4 °C and visualized using phosphorimaging.

Preparation of Nuclear, Cytoplasmic, and Total-Cell Fraction. Total, nuclear, and cytoplasmic fractions were isolated from HeLa and SK-N-MC cells (4×10^6) using NE-PER Nuclear Cytoplasmic Extraction Kit (Thermo Scientific) according to the manufacturer instructions. RNA was purified from each fraction using TRIzol Reagent (Invitrogen).

1. Monshausen M, Gehring NH, Kosik KS (2004) The mammalian RNA-binding protein Staufen2 links nuclear and cytoplasmic RNA processing pathways in neurons. *Neuromolecular Med* 6(2-3):127–144.
2. Miki T, et al. (2011) Cell type-dependent gene regulation by Staufen2 in conjunction with Upf1. *BMC Mol Biol* 12:48.
3. Kim YK, Furic L, DesGroseillers L, Maquat LE (2005) Mammalian Staufen1 recruits Upf1 to specific mRNA 3′UTRs so as to elicit mRNA decay. *Cell* 120(2):195–208.
4. Kim YK, et al. (2007) Staufen1 regulates diverse classes of mammalian transcripts. *EMBO J* 26(11):2670–2681.
5. Isken O, Maquat LE (2008) The multiple lives of NMD factors: Balancing roles in gene and genome regulation. *Nat Rev Genet* 9(9):699–712.
6. Gong C, Maquat LE (2011) lncRNAs transactivate STAU1-mediated mRNA decay by duplexing with 3′ UTRs via Alu elements. *Nature* 470(7333):284–288.
7. Gong C, Kim YK, Woeller CF, Tang Y, Maquat LE (2009) SMD and NMD are competitive pathways that contribute to myogenesis: Effects on PAX3 and myogenin mRNAs. *Genes Dev* 23(1):54–66.
8. Hwang J, Sato H, Tang Y, Matsuda D, Maquat LE (2010) UPF1 association with the cap-binding protein, CBP80, promotes nonsense-mediated mRNA decay at two distinct steps. *Mol Cell* 39(3):396–409.
9. Kuyumcu-Martinez M, et al. (2004) Calicivirus 3C-like proteinase inhibits cellular translation by cleavage of poly(A)-binding protein. *J Virol* 78(15): 8172–8182.
10. Johannes G, Sarnow P (1998) Cap-independent polysomal association of natural mRNAs encoding c-myc, BiP, and eIF4G conferred by internal ribosome entry sites. *RNA* 4(12):1500–1513.
11. Hosoda N, Kim YK, Lejeune F, Maquat LE (2005) CBP80 promotes interaction of Upf1 with Upf2 during nonsense-mediated mRNA decay in mammalian cells. *Nat Struct Mol Biol* 12(10):893–901.
12. Lejeune F, Maquat LE (2004) Immunopurification and analysis of protein and RNA components of mRNP in mammalian cells. *Methods Mol Biol* 257:115–124.
13. Chamieh H, Ballut L, Bonneau F, Le Hir H (2008) NMD factors UPF2 and UPF3 bridge UPF1 to the exon junction complex and stimulate its RNA helicase activity. *Nat Struct Mol Biol* 15(1):85–93.
14. Chakrabarti S, et al. (2011) Molecular mechanisms for the RNA-dependent ATPase activity of Upf1 and its regulation by Upf2. *Mol Cell* 41(6):693–703.
15. Bonneau F, Basquin J, Ebert J, Lorentzen E, Conti E (2009) The yeast exosome functions as a macromolecular cage to channel RNA substrates for degradation. *Cell* 139(3):547–559.

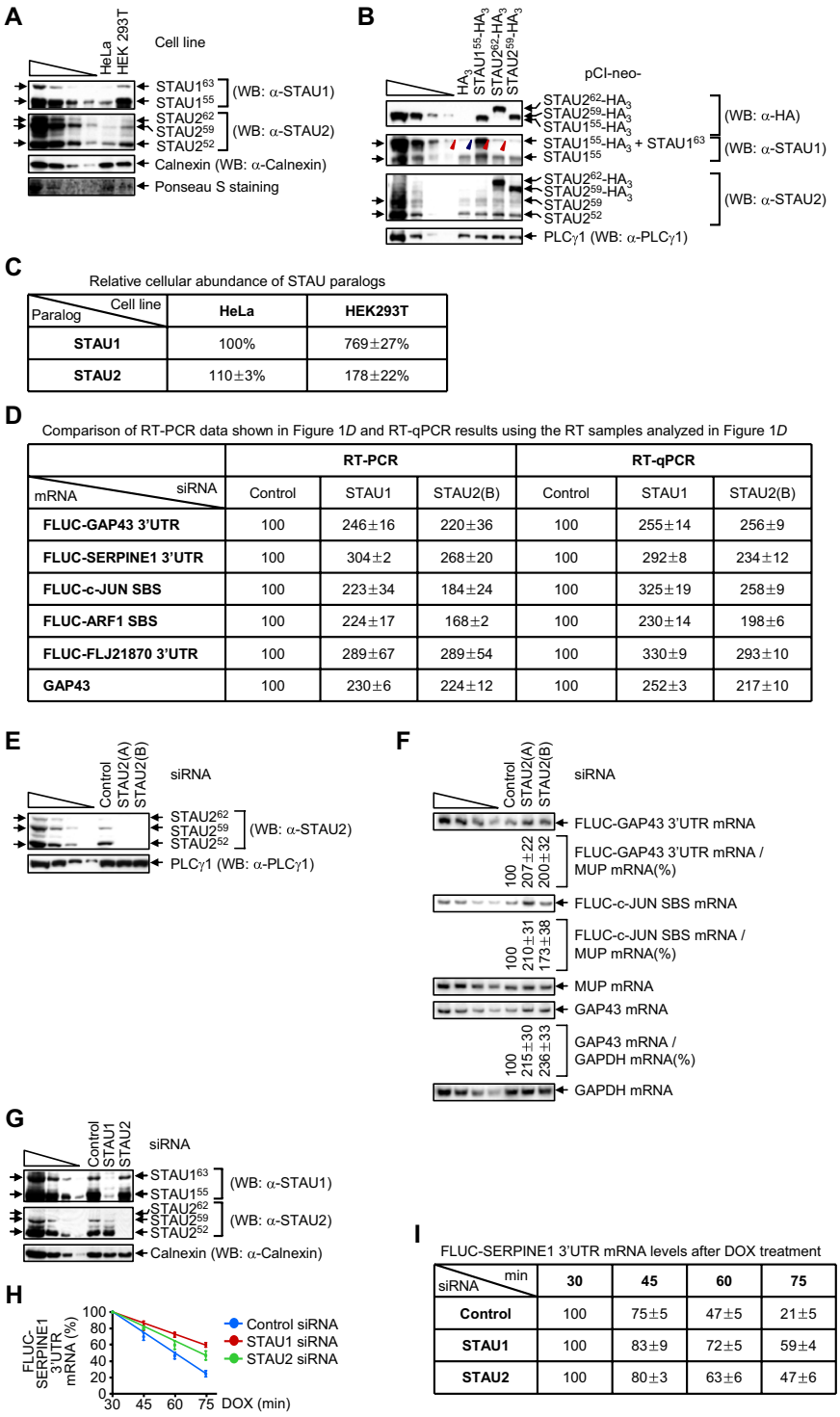

Fig. S1. STAU1 and STAU2 expression levels in HeLa and HEK293T cells, RT-qPCR of samples analyzed in Fig. 1*D*, and analysis of additional STAU2 siRNAs. (*A*) WB was performed using the specified antibody (α) and cell lysates. Calnexin controlled for variations in protein loading, as did Ponceau S-staining. The left-most four lanes show threefold dilutions of HEK293T-cell lysates and indicate that the analyses are semiquantitative. (*B*) WB of proteins analyzed in Fig. 4*A* (i.e., using lysates from HeLa cells expressing an equal amount of $STAU1^{55}$-HA_3, $STAU2^{62}$-HA_3, or $STAU2^{59}$-HA_3). Red arrowheads indicate endogenous $STAU1^{63}$, and the blue arrowhead denotes exogenous $STAU1^{55}$-HA_3 + endogenous $STAU1^{63}$. (*C*) Tabulation of the relative cellular abundance of STAU1 and STAU2 isoforms using data from *A* and *B*. Briefly, using *B*, the level of cellular $STAU1^{55}$ was normalized to the level of $STAU1^{55}$-HA_3 and defined as 100. The level of cellular $STAU2^{59}$ was then normalized to the level of $STAU2^{59}$-HA_3, and the normalized level of $STAU2^{59}$ was then determined as a percentage of the normalized level of cellular $STAU1^{55}$. Using *A*, each STAU1 and STAU2 isoform in HEK293T cells was determined as a percentage of the level of the normalized isoform in HeLa cells. Normalized values represent the sum-total of all isoforms because their ratio is the same in the two cells. (*D*) Comparison of RT-PCR data in Fig. 1*D* and RT-qPCR results obtained using the RT analyzed in Fig. 1*D*, where the level of each reporter SMD target was normalized to the level of MUP mRNA, the level of each cellular SMD target was normalized to the level of its pre-mRNA, and the normalized level of each reporter or cellular SMD target in the presence of Control siRNA was defined as 100. (*E* and *F*) As in Fig. 1 *C* and *D* but using the specified STAU2 siRNA. Arrows pointing right denote STAU isoforms. (*G* and *H*)

Legend continued on following page

HeLa Tet-Off Advanced cells (6×10^5 per 60-mm dish) were transiently transfected with the specified siRNA in the presence of 2 μg/mL of doxycycline (DOX) and, after removing DOX 48 h later, were transfected with 1 μg of the pTRE-FLUC-SERPINE1 3′ UTR test plasmid (1), which is similar to pcFLUC-SERPINE1 3′ UTR except test-gene expression is driven by the DOX-repressible TRE promoter, and 0.5 μg of phCMV-MUP. A fraction of cells was harvested after an additional 4 h (time 0), at which point 2 μg/mL of DOX was added to the remaining cells. Additional fractions of cells were harvested at the specified times thereafter. (*G*) WB essentially as in *C*. (*H*) RT-qPCR, where the level of each FLUC-SERPINE1 3′ UTR mRNA at each time point was normalized to the level of MUP mRNA. Normalized levels were presented as a percentage of the normalized level at 30 min, which was defined as 100. (*I*) Tabulation of the RT-qPCR data shown in *H*. Results are representative of at least three independently performed experiments that did not vary by more than the amount shown.

1. Gong C, Maquat LE (2011) lncRNAs transactivate STAU1-mediated mRNA decay by duplexing with 3′ UTRs via Alu elements. *Nature* 470(7333):284–288.

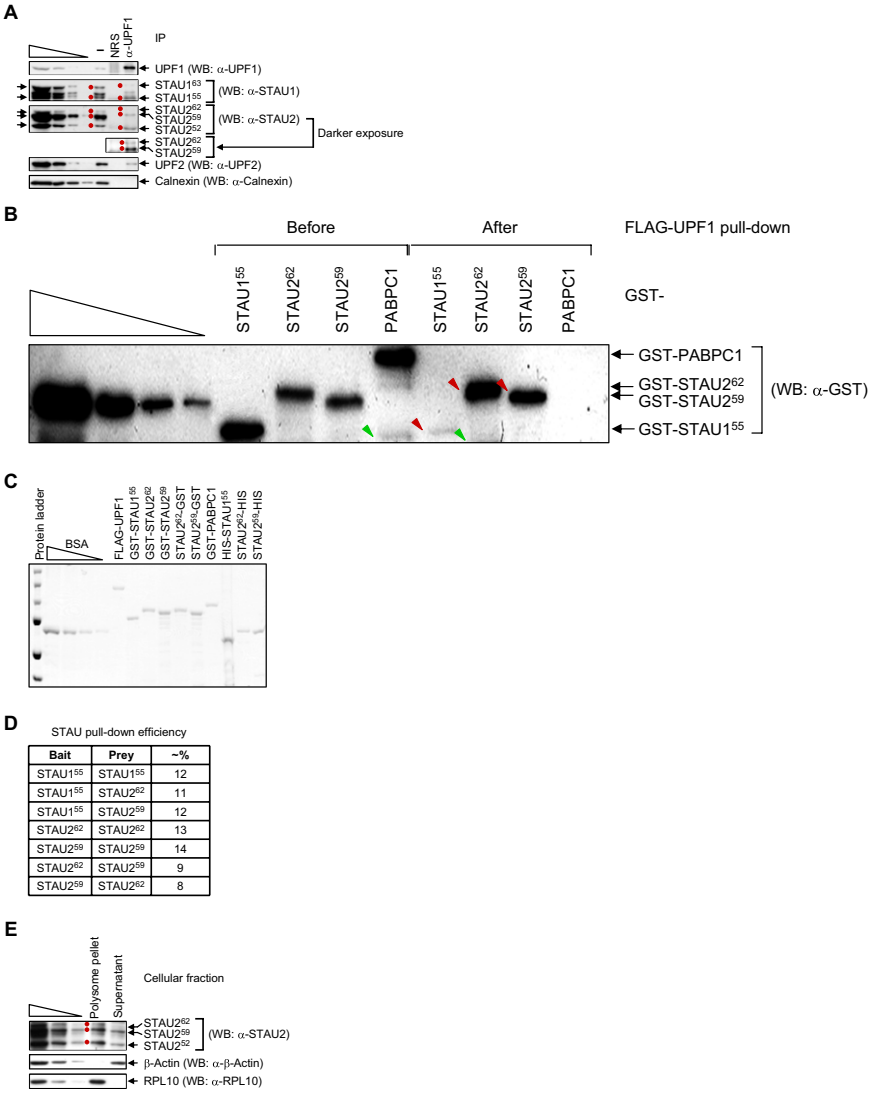

Bait	Prey	~%
STAU1^{55}	STAU1^{55}	12
STAU1^{55}	STAU2^{62}	11
STAU1^{55}	STAU2^{59}	12
STAU2^{62}	STAU2^{62}	13
STAU2^{59}	STAU2^{59}	14
STAU2^{62}	STAU2^{59}	9
STAU2^{59}	STAU2^{62}	8

Fig. S2. Cellular STAU2^{62} and STAU2^{59} coimmunoprecipitate with cellular UPF1 in SK-N-MC cells that were cross-linked using formaldehyde before lysis, indicating that the interactions occur in vivo and are not experimental artifacts. (*A*) As in Fig. 2*A*, except lysates from formaldehyde-cross-linked SK-N-MC cells were analyzed using WB before (–) or after IP using anti(α)-UPF1 or, as a negative control, normal rabbit serum (NRS). (*B*) Enlargement of Fig. 2*B* that illustrates the difference in mobility between those GST-STAU proteins under analysis and degradation products that derive from either GST-PABPC1 before pull-down or GST-STAU2^{62} after pull-down, each of which is denoted with a green arrowhead. (*C*) Coomassie blue-staining of SDS-polyacrylamide-separated FLAG-UPF1, GST-STAU1^{55}, GST-STAU2^{62}, GST-STAU2^{59}, STAU2^{62}-GST, STAU2^{59}-GST, GST-PABPC1, HIS-STAU1^{55}, STAU2^{62}-HIS, and STAU2^{59}-HIS, each of which was produced in *E. coli*. The protein ladder (Bio-Rad) provides molecular-weight standards. Lanes 2–5 from the left consist of a twofold serial dilution of BSA. (*D*) Percentage (%) of the specified cellular prey that was pulled down by the specified bait using data in Fig. 3 *A*–*C*. (*E*) Western blotting of the specified SK-N-MC-cell fractions demonstrates that all three STAU2 isoforms are polysome-associated, in contrast to the finding by Duchaîne et al. (1) that, of the three, STAU2^{62} is not. Arrows pointing right and red dots denote STAU isoforms. Results are representative of at least two independently performed experiments.

1. Duchaîne TF, et al. (2002) Staufen2 isoforms localize to the somatodendritic domain of neurons and interact with different organelles. *J Cell Sci* 115(Pt 16):3285–3295.

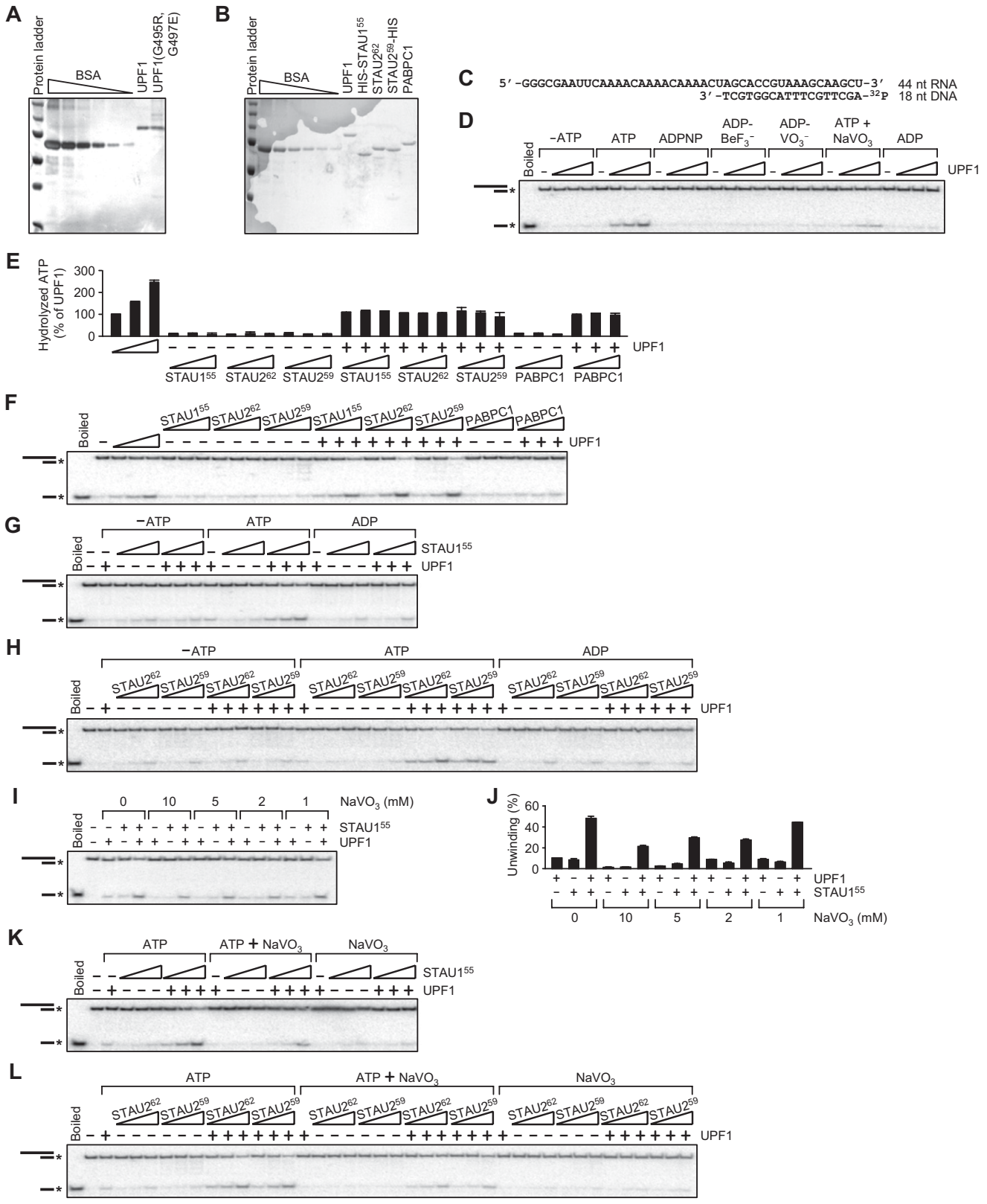

Fig. S3. Proteins and RNA–DNA duplex used in the ATPase and helicase assays in Fig. 6, and data shown in Fig. 6 *F, H–J, L,* and *M*. (*A*) Visualization of SDS-polyacrylamide-separated human UPF1 and UPF1(G495R,G497E) proteins produced in *E. coli* using SYPRO Ruby Protein Gel Stain. (*B*) Coomassie blue-staining of SDS-polyacrylamide-separated UPF1, HIS-STAU1^{55}, STAU2^{62}, STAU2^{59}-HIS, and PABPC1. The protein ladder (Bio-Rad) provides molecular-weight standards. Lanes 2–7 from the left consist of a twofold serial dilution of BSA. (*C*) Sequence of the RNA–DNA duplex with a 5′-ssRNA overhang used in helicase assays. (*D*) Data correspond to Fig. 6*F*. (*E*) As in Fig. 6*G* except that 0.25 nM of γ-[^{32}P]-labeled RNA–DNA duplex was used instead of poly(U). (*F*) Data correspond to Fig. 6*H*. (*G*) Data correspond to Fig. 6*I*. (*H*) Data correspond to Fig. 6*J*. (*I*) Helicase assays and (*J*) corresponding histograms demonstrating the effect of different $NaVO_3$ concentrations on HIS-STAU1^{55}-stimulated UPF1 unwinding in the presence of 2 mM of ATP. (*K*) Data correspond to Fig. 6*L*. (*L*) Data correspond to Fig. 6*M*.

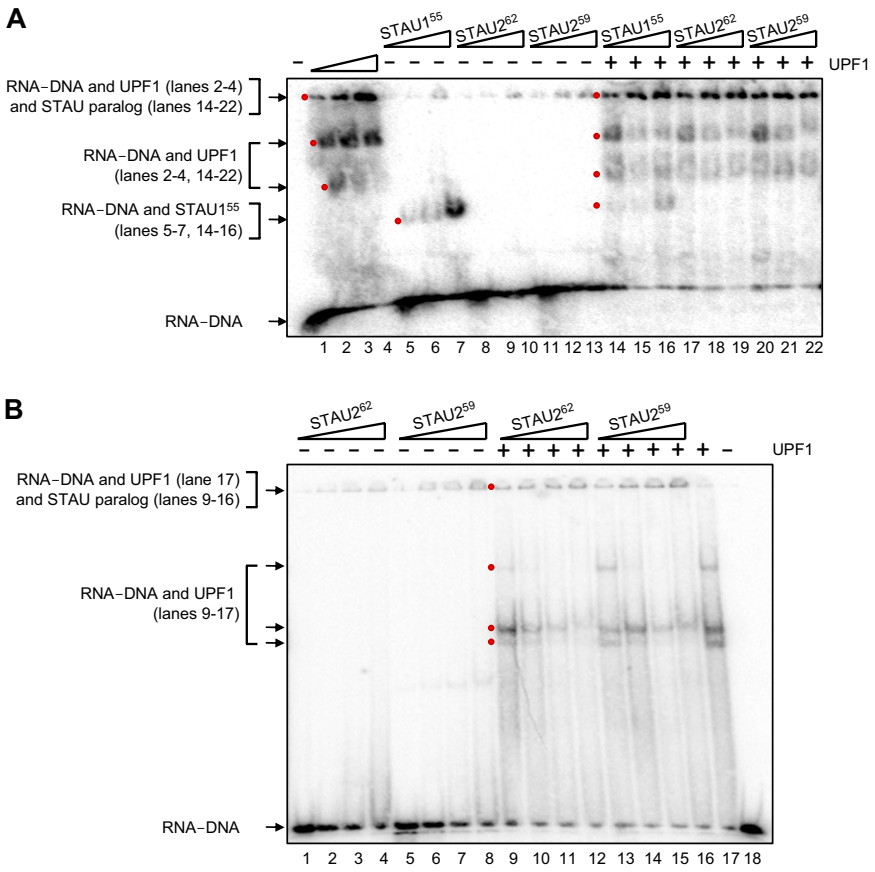

Fig. S4. EMSA demonstrating that STAU1 but not STAU2 binds the RNA–DNA duplex used in the helicase assays and ATPase assays of Fig. S3*E*. (*A*) RNA–DNA duplex and protein-binding assays using 0 (–), 40, 80, or 160 nM (wedge) of UPF1 or 40 nM of UPF1 (+) and/or 40, 80, or 160 nM (wedge) of HIS-STAU1^{55}, STAU2^{62}, or STAU2^{59}-HIS in the presence of 1 nM of γ-[^{32}P]-labeled RNA–DNA duplex. Mobilities of the RNA–DNA duplex and RNA–DNA duplex bound by particular proteins are described to the left. Red dots align with arrows. (*B*) As in *A*. However, these RNA–DNA duplex and protein-binding assays used 0 (–), or 40 nM of UPF1 (+) and/or 40, 80, 160, or 320 nM (wedge) of STAU2^{62} or STAU2^{59}-HIS in the presence of 1 nM of γ-[^{32}P]-labeled RNA–DNA duplex.

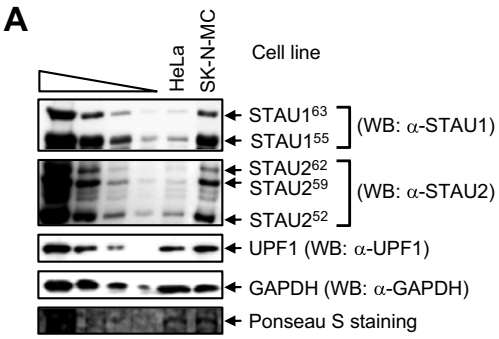

B Relative cellular abundance of STAU paralogs

Paralog \ Cell line	HeLa	SK-N-MC
STAU1	100%	798±18%
STAU2	110±3%	608±35%

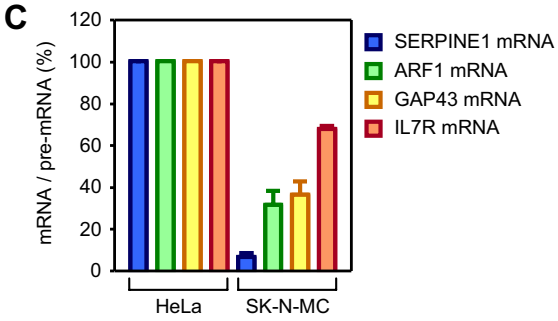

D Cytoplasmic and nuclear distribution of SMD targets in HeLa and SK-N-MC cell lines

Cell line / mRNA	HeLa		SK-N-MC	
	Cyt (%)	Nuc (%)	Cyt (%)	Nuc (%)
SERPINE1	99.8	0.2	99.2	0.8
GAP43	97.7	2.3	98.7	1.3
ARF1	97.5	2.5	97.7	2.3
IL7R	99.5	0.5	99.1	0.9

Fig. S5. The cytoplasmic abundance of STAU1 together with STAU2 determines the efficiency of SMD: a comparison of HeLa and SK-N-MC cells. (*A*) HeLa or SK-*N*-MC cells (3×10^7 per 150-mm dish) were lysed and total-cell, cytoplasmic, and nuclear fractions were generated. Total-cell lysates were analyzed by WB using the specified antibody (α). GAPDH and Ponceau S-staining controlled for variations in protein loading. The left-most four lanes show threefold dilutions of lysates from SK-N-MC cells. (*B*) Using data from Fig. S1*C* and Fig. S5*A*, tabulation of the relative total-cell abundance of STAU1 and STAU2 in HeLa and SK-N-MC cells. (*C*) RT-qPCR of SERPINE1, ARF1, GAP43, and IL7R mRNAs and pre-mRNAs in total-cell RNA. Each mRNA was normalized to the level of pre-mRNA, and the normalized level of each mRNA in HeLa cells was defined as 100. (*D*) Tabulation of the cytoplasmic and nuclear distribution of each mRNA analyzed in *C* shows that the relatively efficient SMD in SK-N-MC cells compared with HeLa cells is not due to differences in the cellular distribution of those mRNAs analyzed, which would change their accessibility to cellular factors required for SMD. Results of at least three independently performed experiments did not vary by more than the amount shown.